Modeling and Hierarchical Tracking Control of Tri-Wheeled Mobile Robots

Pu-Sheng Tsai, Li-Sheng Wang, and Fan-Ren Chang

***Abstract*—After exploring the structure of the dynamics derived by using the Appell equation, we propose a hierarchical tracking controller for a tri-wheeled mobile robot in this paper. With appropriately chosen privileged variables, the reduced equations are decoupled from the kinematic equations associated with the underlying nonholonomic constraints. This special character of the system makes it possible to separate the design into three levels: motion planning, kinematic, and dynamic. In the proposed scheme, a fuzzy inference engine in the kinematic level is used to update the desired trajectory computed in the motion-planning level. An adaptive sliding-mode controller is then adopted to track the new reference values of privileged variables in the dynamic level, which subsequently drives the nonprivileged variables. Simulation results show the effectiveness of such a tracking-control scheme, which concurrently takes kinematics and dynamics into consideration. All system variables can be tracked asymptotically to their desired values, which are assured by the skew-symmetric property of the Appell equation.**

***Index Terms*—Hierarchical tracking control, nonholonomic constraint, privileged coordinates, reduced Appell equation, skew-symmetric property.**

I. Introduction

For a vehicle or a mobile robot moving with nonsliding rolling wheels, problems associated with nonholonomic constraints naturally arise. To deal with the motion planning of a nonholonomic system, the subject of nonholonomic motion planning (NMP) has been studied extensively [1], in which various algorithms [2], [3] have been developed to generate a feasible trajectory satisfying the nonholonomic constraints. Moreover, the kinematic equations are sometimes treated as a control problem, and one tries to design the so-called kinematic controller, in which discontinuous feedback [4], [5], time-varying feedback [6], [7], or hybrid feedback [8] may be used. However, ignoring the mass and the moment of inertia of the system, which appear in the dynamic equations, may lead to the inability of following the generated trajectory effectively.

In robot motion control, torque commands enter through the dynamical equations; therefore, it is desirable to design the controller based upon the combined kinematic and dynamic equations. In [9], a kinematic controller and a neural network computed torque controller are integrated to stabilize a nonholonomic mobile robot in which uncertainty exists. The point stabilization problems were solved in [10] and [11] by first transforming the kinematic equation into a skew-symmetric chained form, and then designing the adaptive controller for the combined system. In [12], a robust damping control scheme is proposed. Nevertheless, most of the previous works adopted Lagrangian formulation, in which Lagrange's multipliers are included in the dynamical equation to deal with the kinematic constraints. The complexity of the problem is then raised, and the failure of the kinematic constraints may occur in numerical computation. While the projection method may be used to reduce the number of equations, a systematic approach which explores the intrinsic structure of the system may lead to a favorable form of the reduced equations. The methodology proposed in this paper serves as an example, and, based on which, the controller design may be made more effective.

Among many fundamental equations in mechanics, such as the D'Alembert–Lagrange equation, the Gibbs–Appell equation, and the Boltzmann–Hamel equations, etc., cf. [13], the Jourdain variational equation [14] in virtual velocities is more suitable to be used to treat the kinematic (velocity) constraints. In a recent paper [15], the Jourdain equation was applied to systematically derive the Appell equation, which is analogous to the equation obtained by using Kane's approach [16]. In the method, the generalized coordinates are divided into two sets, one for privileged coordinates, and the other for nonprivileged coordinates. It was further noted that if the system is reducible, in the sense that the nonprivileged variables do not appear in the Appell equation, the reduced dynamical equation is decoupled from the kinematic equation.

By extending the results of [15], we establish in Section III a systematic and structural procedure to derive the reduced dynamical equations in matrix form. The equations of motion of a tri-wheeled mobile robot described in Section II are then derived. For coupled multibody systems, this approach reduces the complexity significantly over conventional methods, such as Lagrangian formulism. Moreover, if the system is reducible, we may design a controller for the reduced dynamics to steer the privileged coordinates without interlacing with the kinematics. Based on this structure, the proposed hierarchical tracking control discussed in Section IV is composed of three levels. On the top, according to mission requirements, NMP methods are employed to generate a feasible path where the kinematic constraints are satisfied. The desired trajectories of the privileged variables are, however, changed in the middle level by a kinematic compensator, according to the current configuration of the system. The updated values are then fed into the dynamic controller in the bottom level. Equipped with a good kinematic compensator and dynamic controller, the proposed scheme can produce an effective tracking controller for nonholonomically constrained mechanical systems.

After suitably choosing the privileged velocities, the system of a tri-wheeled mobile robot is rendered reducible, and the above-described methodology is applicable. A fuzzy logic system is used to implement the kinematic compensator, and an adaptive sliding-mode controller is adopted in the dynamic level to accommodate uncertain parameters. The latter is possible due to the fact that the reduced Appell equation satisfies the skew-symmetric property, as proved in Section III. Simulation results presented in Section V demonstrate the performance of the proposed controller, which can indeed drive the system variables defined in Section IV to follow the desired trajectory asymptotically.

II. Problem Description

The problem to be solved here is the tracking of a desired trajectory for a tri-wheeled mobile robot moving on a horizontal plane, as depicted in Fig. 1. The system may be modeled by a platform (body 4) with mass m_p, width w, and length l, attached by two fixed rear wheels (body 1 and 2) and one steering front wheel (body 3) of the same mass m_w and radius a, cf. Fig. 2. The masses of the rim of the wheel and the edge of the platform are denoted by m_w' and m_p', respectively. Let $2b$ denote the distance between the two rear wheels, and ρ_f, ρ_r be the respective distances from the mass center of the platform C_4 to that

Manuscript received March 31, 2005; revised November 4, 2005. This paper was recommended for publication by Associate Editors N. Sarkar and B. J. Yi and Editors S. Hutchinson and L. Parker upon evaluation of the reviewers' comments. The work was supported in part by the National Science Council of the Republic of China (Taiwan) under Grants NSC-93-2212-E-002-026 and NSC-93-2213-E-002-052. This paper was presented in part at the 44th IEEE Conference on Decision and Control, Seville, Spain, December 2005.

P.-S. Tsai and F.-R. Chang are with the Department of Electrical Engineering, National Taiwan University, Taipei, Taiwan, R.O.C. (e-mail: elaine@cc.chit.edu.tw; frchang@ac.ee.ntu.edu.tw).

L.-S. Wang is with the Institute of Applied Mechanics, National Taiwan University, Taipei, Taiwan, R.O.C. (e-mail: wangli@iam.ntu.edu.tw).

Digital Object Identifier 10.1109/TRO.2006.878964

1552-3098/$20.00 © 2006 IEEE

Authorized licensed use limited to: National Taiwan University. Downloaded on December 19, 2008 at 02:28 from IEEE Xplore. Restrictions apply.

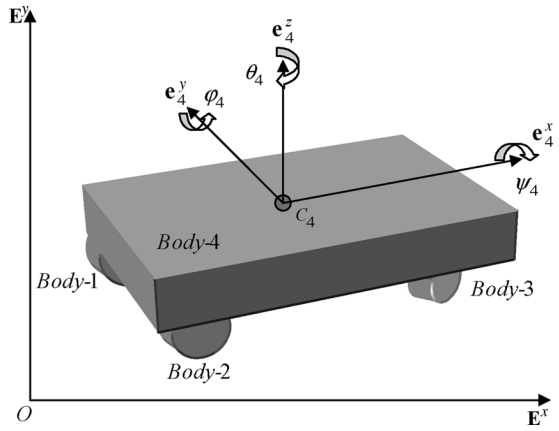

Fig. 1. Three-wheeled mobile robot.

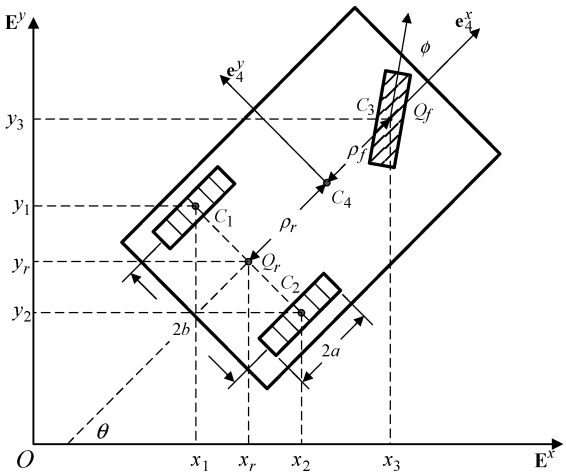

Fig. 2. Configuration of the mobile robot.

of front wheel C_3 and the center of the rear axle Q_r. The contacts between the wheels and the plane are assumed to be pure rolling without side slipping.

Let $\{\mathbf{E}^x, \mathbf{E}^y, \mathbf{E}^z\}$ be an inertial frame fixed to the plane. The translational motion of body i $(i = 1, 2, 3, 4)$ may be described by the position of its mass center

$$\mathbf{r}_i^C = x_i \mathbf{E}^x + y_i \mathbf{E}^y + z_i \mathbf{E}^z. \tag{1}$$

For the rotational motion, type (3-1-2) Eulerian angles are used such that the inertial frame is rotated to $\{\mathbf{i}_i', \mathbf{j}_i', \mathbf{k}_i' = \mathbf{E}^z\}$ by the heading angle θ_i, then to $\{\mathbf{i}_i'' = \mathbf{i}_i', \mathbf{j}_i'', \mathbf{k}_i''\}$ by the camber angle ψ_i, and finally to the body-fixed frame $\{\mathbf{e}_i^x, \mathbf{e}_i^y = \mathbf{j}_i'', \mathbf{e}_i^z\}$ by the spin angle φ_i. If the rotation is time-varying, the rates of change of the Eulerian angles are related to the angular velocity $\boldsymbol{\omega}_i$ by

$$\boldsymbol{\omega}_i = \dot{\theta}_i \mathbf{E}^z + \dot{\psi}_i \mathbf{i}_i' + \dot{\varphi}_i \mathbf{j}_i'', \quad i = 1, 2, 3, 4. \tag{2}$$

From the geometry of the system, the moments of inertia can be found to be

$$\mathbf{J}_i = \frac{1}{2} m_w' a^2 \mathbf{i}_i' \mathbf{i}_i' + m_w' a^2 \mathbf{j}_i' \mathbf{j}_i' + \frac{1}{2} m_w' a^2 \mathbf{k}_i' \mathbf{k}_i', \quad i = 1, 2, 3 \tag{3}$$

$$\mathbf{J}_4 = \frac{1}{3} m_p' w^2 \mathbf{i}_4' \mathbf{i}_4' + \frac{1}{3} m_p' l^2 \mathbf{j}_4' \mathbf{j}_4' + \frac{1}{3} m_p' (w^2 + l^2) \mathbf{k}_4' \mathbf{k}_4'. \tag{4}$$

The six variables $(x_i, y_i, z_i, \psi_i, \varphi_i, \theta_i)$ are used here to describe the configuration of body i, and therefore, there are 24 coordinates to be specified for the system. However, due to physical constraints, the number may be reduced. Since the motion is horizontal, we have $z_1 = z_2 = z_3 = a$ and $z_4 = h$. The assumption that the platform is kept horizontal yields $\varphi_4 = \psi_4 = 0$, and hence, the body frame $\{\mathbf{e}_4^x, \mathbf{e}_4^y, \mathbf{e}_4^z\}$ coincides with $\{\mathbf{i}_4'', \mathbf{j}_4'', \mathbf{k}_4''\}$ and $\{\mathbf{i}_4', \mathbf{j}_4', \mathbf{k}_4'\}$. If the wheels are properly aligned, the camber angles for the wheels are zeros, i.e., $\psi_1 = \psi_2 = \psi_3 = 0$, so that $\{\mathbf{i}_i'', \mathbf{j}_i'', \mathbf{k}_i''\}$ coincides with $\{\mathbf{i}_i', \mathbf{j}_i', \mathbf{k}_j'\}$, for $i = 1, 2, 3$. Moreover, it is assumed that the vehicle is driven by the front wheel. Additional constraints on the heading angles of the platform and rear wheels are thus imposed as $\theta_1 = \theta_2 = \theta_4 (\equiv \theta)$. The geometry of the interconnected bodies (cf. Fig. 2) further requires that

$$\begin{aligned} x_1 &= x_3 - \rho\cos\theta - b\sin\theta, \quad & y_1 &= y_3 - \rho\sin\theta + b\cos\theta, \\ x_2 &= x_3 - \rho\cos\theta + b\sin\theta, \quad & y_2 &= y_3 - \rho\sin\theta - b\cos\theta, \\ x_4 &= x_3 - \rho\cos\theta + \rho_r\cos\theta, \quad & y_4 &= y_3 - \rho\sin\theta + \rho_r\sin\theta \end{aligned}$$

where $\rho = \rho_r + \rho_f$. Finally, the conditions that the wheels roll without slipping is realized by the following velocity constraints:

$$\begin{aligned} \dot{x}_1 &= a\dot{\varphi}_1\cos\theta, & \dot{y}_1 &= a\dot{\varphi}_1\sin\theta, \\ \dot{x}_2 &= a\dot{\varphi}_2\cos\theta, & \dot{y}_2 &= a\dot{\varphi}_2\sin\theta, \\ \dot{x}_3 &= a\dot{\varphi}_3\cos(\theta+\phi), & \dot{y}_3 &= a\dot{\varphi}_3\sin(\theta+\phi) \end{aligned} \tag{5}$$

where $\phi (= \theta_3 - \theta)$ denotes the steering angle of the front wheel.

Due to the geometric constraints, the previous set of six velocity constraints is not independent. In term of the coordinates of Q_r, i.e., $x_r = x_3 - \rho\cos\theta$ and $y_r = y_3 - \rho\sin\theta$, which shall be used to describe the motion, the set of constraints in (5) can be converted to the following five independent ones:

$$a\dot{\varphi}_1 + 2b\dot{\theta} = a\dot{\varphi}_2 \tag{6}$$

$$\dot{x}_r\sin\theta - \dot{y}_r\cos\theta = 0 \tag{7}$$

$$\dot{x}_r\cos\theta + \dot{y}_r\sin\theta - b\dot{\theta} = a\dot{\varphi}_1 \tag{8}$$

$$\dot{x}_r\sin(\theta+\phi) - \dot{y}_r\cos(\theta+\phi) - \rho\dot{\theta}\cos\phi = 0 \tag{9}$$

$$\dot{x}_r\cos(\theta+\phi) + \dot{y}_r\sin(\theta+\phi) + \rho\dot{\theta}\sin\phi = a\dot{\varphi}_3. \tag{10}$$

Note that Condition (6) can be integrated to yield a geometric constraint $a\varphi_1 + 2b\theta = a\varphi_2 +$ (a constant). As a result, the system is subject to 18 geometric constraints and 4 nonholonomic constraints. The dimension of the system is, hence, dropped to six, and we choose $(x_r, y_r, \theta, \varphi_1, \varphi_3, \phi)$ to be the generalized coordinates, due to their appearances in (7)–(10). In these generalized coordinates, the angular velocities in (2) can be expressed as

$$\begin{aligned} \boldsymbol{\omega}_1 &= \dot{\theta}\mathbf{E}^z + \dot{\varphi}_1\mathbf{j}_1'' \\ \boldsymbol{\omega}_2 &= \dot{\theta}\mathbf{E}^z + (\dot{\varphi}_1 + 2b\dot{\theta}/a)\mathbf{j}_2'' \\ \boldsymbol{\omega}_3 &= (\dot{\theta} + \dot{\phi})\mathbf{E}^z + \dot{\varphi}_3\mathbf{j}_3'' \\ \boldsymbol{\omega}_4 &= \dot{\theta}\mathbf{E}^z. \end{aligned} \tag{11}$$

Based on the above framework, the desired trajectory to be tracked may be specified by $(x_{rd}(t), y_{rd}(t), \theta_d(t), \varphi_{1d}(t), \varphi_{3d}(t), \phi_d(t))$, for $t \in (0, t_f)$. To achieve the objective of trajectory tracking, two control torques τ_1 and τ_2 are exerted on the spin and steering angle of the front wheel, respectively. The torques affect the motion through the dynamical equations, which shall be derived below by using the Appell equation.

Authorized licensed use limited to: National Taiwan University. Downloaded on December 19, 2008 at 02:28 from IEEE Xplore. Restrictions apply.

III. Reduced Appell Equation

A. Reduced Appell Equation for Coupled Rigid Bodies

Consider a mechanical system consisting of N interconnected rigid bodies. The motion of body j with mass m_j may be described by the translation of its mass center C_j, $\mathbf{r}_j^C(t) = [x_j(t)y_j(t)z_j(t)]^T$, $j = 1, 2, \ldots, N$, and a rotation about C_j represented by $\Phi_j(t) \in \mathrm{SO}(3)$, the special orthogonal group, satisfying $\Phi_j \cdot \Phi_j^c = \mathbf{1}$, $\det \Phi_j = 1$ (in dyadic notation, cf. [17]). Here Φ_j^c denotes the conjugate of Φ_j, and $\mathbf{1}$ is the identity dyadic. For time-varying rotations with angular velocity $\boldsymbol{\omega}_j$, we have

$$\dot{\Phi}_j = \boldsymbol{\omega}_j \times \Phi_j = (\mathbf{1} \times \boldsymbol{\omega}_j) \cdot \Phi_j. \tag{12}$$

If the system is subject to K independent geometric constraints, the dimension of the system becomes $n = 6N - K$, and we may be able to express the position and attitude of each body in terms of the generalized coordinates $\mathbf{q} = [q_1, q_2, \ldots, q_n]^T$, i.e., $\mathbf{r}_j^C = \hat{\mathbf{r}}_j^C(\mathbf{q})$, $\Phi_j = \hat{\Phi}_j(\mathbf{q})$. By taking time derivatives, we obtain

$$\dot{\mathbf{r}}_j^C = \sum_{r=1}^{n} \frac{\partial \hat{\mathbf{r}}_j^C}{\partial q_r}(\mathbf{q})\dot{q}_r, \quad \dot{\Phi}_j = \sum_{r=1}^{n} \frac{\partial \hat{\Phi}_j}{\partial q_r}(\mathbf{q})\dot{q}_r. \tag{13}$$

From (12) and the second equation in (13), the $\boldsymbol{\omega}_j$ can be expressed as

$$\boldsymbol{\omega}_j = \sum_{r=1}^{n} \mathrm{Axial}\left[\frac{\partial \hat{\Phi}_j}{\partial q_r}(\mathbf{q}) \cdot \hat{\Phi}_j^c(\mathbf{q})\right] \dot{q}_r \tag{14}$$

where $\mathrm{Axial}[\cdot]$ denotes the axial vector of a skew-symmetric dyadic (tensor).

If the system is further constrained by L independent nonholonomic conditions, the generalized velocities $\dot{q}_r$, $r = 1, \ldots, n$, may be related by

$$\sum_{r=1}^{n} D_{sr}\left(\hat{\mathbf{r}}^C(\mathbf{q}), \hat{\boldsymbol{\Phi}}(\mathbf{q})\right)\dot{q}_r = 0, \quad s = 1, 2, \ldots, L. \tag{15}$$

Let $\mathbf{D} \in R^{L \times n}$ denote the matrix formed by the coefficients D_{sr}. Due to the independence of the constraints, the matrix $\mathbf{D}$ is of full rank, so that the degree of freedom of the system becomes $m = n - L$. One may now choose m independent generalized velocities, say $\dot{y}_k$, $k = 1, 2, \ldots, m$, which shall be called the *privileged velocities*, so that some column operations may be performed to decompose $\mathbf{D}$ into two parts: a nonsingular matrix $\mathbf{D}' \in R^{L \times L}$, and $\mathbf{D}'' \in R^{L \times m}$. Denoting the remaining generalized velocities as $\dot{z}_s$, $s = 1, 2, \ldots, L$, termed the *nonprivileged velocities*, (15) can be rewritten as

$$\dot{z}_s = \sum_{k=1}^{m} B_{sk}\dot{y}_k, \quad s = 1, 2, \ldots, L, \left(B_{sk} = -\sum_{h=1}^{L} (\mathbf{D}')_{sh}^{-1} D''_{hk}\right). \tag{16}$$

Conceptually, the generalized coordinates refer to independent *coordinates* corresponding to the geometric constraints, whereas the privileged velocities are the independent *velocities* with respect to the nonholonomic constraints. The term "privileged coordinate" has been used in [18] to represent independent coordinates in the set of Lagrangian coordinates and quasi-coordinates.

Under this setting, the generalized velocities can be expressed as

$$\dot{q}_r = \sum_{k=1}^{m} A_{rk}\dot{y}_k, \quad r = 1, 2, \ldots, n. \tag{17}$$

By substituting (17) into (13) and (14), we obtain

$$\dot{\mathbf{r}}_j^C = \sum_{k=1}^{m} \boldsymbol{\gamma}_{jk}(\mathbf{y}, \mathbf{z})\dot{y}_k, \quad \boldsymbol{\omega}_j = \sum_{k=1}^{m} \varpi_{jk}(\mathbf{y}, \mathbf{z})\dot{y}_k \tag{18}$$

where

$$\boldsymbol{\gamma}_{jk} = \sum_{r=1}^{n} \frac{\partial \hat{\mathbf{r}}_j^C}{\partial q_r} A_{rk}$$
$$\varpi_{jk} = \sum_{r=1}^{n} \mathrm{Axial}\left[\frac{\partial \hat{\Phi}_j}{\partial q_r}(\mathbf{q}) \cdot \hat{\Phi}_j^c(\mathbf{q})\right] A_{rk} \tag{19}$$

are functions of $\mathbf{y}$ and $\mathbf{z}$ in general. Taking the time derivative of (18), the accelerations can be expressed as

$$\ddot{\mathbf{r}}_j^C = \sum_{k=1}^{m} (\dot{\boldsymbol{\gamma}}_{jk}\dot{y}_k + \boldsymbol{\gamma}_{jk}\ddot{y}_k), \quad \dot{\boldsymbol{\omega}}_j = \sum_{k=1}^{m} (\dot{\varpi}_{jk}\dot{y}_k + \varpi_{jk}\ddot{y}_k). \tag{20}$$

Now the Appell equation derived in [15] is invoked to establish the equations of motion, for $k = 1, 2, \ldots, m$

$$\sum_{j=1}^{N} \left(m_j \ddot{\mathbf{r}}_j^C(\mathbf{q}, \dot{\mathbf{q}}, \ddot{\mathbf{y}}) - \mathbf{F}_j^a\right) \cdot \boldsymbol{\gamma}_{jk}(\mathbf{q}) + \left(\mathbf{J}_j \cdot \dot{\boldsymbol{\omega}}_j + \boldsymbol{\omega}_j \times \mathbf{J}_j \cdot \boldsymbol{\omega}_j - \mathbf{T}_j^a\right)(\mathbf{q}, \dot{\mathbf{q}}, \ddot{\mathbf{y}}) \cdot \varpi_{jk}(\mathbf{q}) = 0. \tag{21}$$

Here, $\mathbf{F}_j^a$ denotes the total applied force, $\mathbf{T}_j^a$ is the total applied moment about C_j, and the moment of inertia about C_j can be expressed in dyadic form as

$$\mathbf{J}_j = \int_{B_j} \left(\left(\mathbf{r}_j' \cdot \mathbf{r}_j'\right)\mathbf{1} - \mathbf{r}_j'\mathbf{r}_j'\right) dm_j = \int_{B_j} \left(\mathbf{1} \times \mathbf{r}_j'\right)^c \cdot \left(\mathbf{1} \times \mathbf{r}_j'\right) dm_j \tag{22}$$

where $\mathbf{r}_j'$ denotes the relative position vector from C_j to the position of the mass element dm_j. In this final form, this set of Appell equations is, in fact, equivalent to the so-called Kane equation in the literature, cf. [19], which is deemed very useful in dealing with complex multibody systems.

If (21) contains only the privileged variables, the system is called *reducible*, in the sense that the dynamic equation for the privileged variables is decoupled from the kinematic conditions (16). Such decoupling paves the way for the design of hierarchical controller proposed in this paper.

B. Reduced Appell Equation in Matrix Form

For a reducible system, the Appell equation (21) can be expressed in matrix form as

$$\mathbf{M}(\mathbf{y})\ddot{\mathbf{y}} + \mathbf{C}(\mathbf{y}, \dot{\mathbf{y}})\dot{\mathbf{y}} = \mathbf{T}(\mathbf{y}) \tag{23}$$

where the components of the matrices are

$$M_{rs} = \sum_{j=1}^{N} (m_j \boldsymbol{\gamma}_{jr} \cdot \boldsymbol{\gamma}_{js} + \varpi_{jr} \cdot \mathbf{J}_j \cdot \varpi_{js}) \tag{24}$$

$$C_{rs} = \sum_{j=1}^{N} \left(m_j \dot{\boldsymbol{\gamma}}_{js} \cdot \boldsymbol{\gamma}_{jr} + \dot{\varpi}_{js} \cdot \mathbf{J}_j \cdot \varpi_{jr} + \sum_{k=1}^{m} \varpi_{jr} \cdot (\varpi_{jk} \times \mathbf{J}_j \cdot \varpi_{js})\dot{y}_k\right) \tag{25}$$

$$T_r = \sum_{j=1}^{N} \left(\mathbf{F}_j^a \cdot \boldsymbol{\gamma}_{jr} + \mathbf{T}_j^a \cdot \varpi_{jr}\right). \tag{26}$$

This set of equations possesses the following intrinsic properties.

Lemma 1: $\mathbf{M}(\mathbf{y})$ is an $m \times m$ positive-definite symmetric matrix.

Lemma 2: The matrix $\boldsymbol{\Pi} = \dot{\mathbf{M}}(\mathbf{y}) - 2\mathbf{C}(\mathbf{y}, \dot{\mathbf{y}})$ is skew-symmetric.

Authorized licensed use limited to: National Taiwan University. Downloaded on December 19, 2008 at 02:28 from IEEE Xplore. Restrictions apply.

Proof: From (24) and (25), we obtain

$$\begin{aligned}\Pi_{rs} &= \sum_{j=1}^{N}(m_j\dot{\boldsymbol{\gamma}}_{jr}\cdot\boldsymbol{\gamma}_{js} - m_j\boldsymbol{\gamma}_{jr}\cdot\dot{\boldsymbol{\gamma}}_{js}) \\ &\quad + \sum_{j=1}^{N}(\dot{\boldsymbol{\varpi}}_{jr}\cdot\mathbf{J}_j\cdot\boldsymbol{\varpi}_{js} - \boldsymbol{\varpi}_{jr}\cdot\mathbf{J}_j\cdot\dot{\boldsymbol{\varpi}}_{js}) \\ &\quad + \sum_{j=1}^{N}\boldsymbol{\varpi}_{jr}\cdot\dot{\mathbf{J}}_j\cdot\boldsymbol{\varpi}_{js} - 2\sum_{j=1}^{N}\sum_{k=1}^{m}\boldsymbol{\varpi}_{jr}\cdot(\boldsymbol{\varpi}_{jk}\times\mathbf{J}_j)\cdot\boldsymbol{\varpi}_{js}\dot{y}_k.\end{aligned} \tag{27}$$

The time derivative of $\mathbf{J}_j$ can be derived from (22) as

$$\begin{aligned}\dot{\mathbf{J}}_j &= \int_{B_j}\left[(\mathbf{1}\times\boldsymbol{\omega}_j)\cdot\left(\mathbf{1}\times\mathbf{r}_j'\right) - \left(\mathbf{1}\times\mathbf{r}_j'\right)\cdot(\mathbf{1}\times\boldsymbol{\omega}_j)\right]^c\cdot\left(\mathbf{1}\times\mathbf{r}_j'\right)dm_j \\ &\quad + \int_{B_j}\left(\mathbf{1}\times\mathbf{r}_j'\right)^c\cdot\left[(\mathbf{1}\times\boldsymbol{\omega}_j)\cdot\left(\mathbf{1}\times\mathbf{r}_j'\right)\right. \\ &\qquad \left. - \left(\mathbf{1}\times\mathbf{r}_j'\right)\cdot(\mathbf{1}\times\boldsymbol{\omega}_j)\right]dm_j \\ &= \int_{B_j}(\mathbf{1}\times\boldsymbol{\omega}_j)\cdot\left(\mathbf{1}\times\mathbf{r}_j'\right)^c\cdot\left(\mathbf{1}\times\mathbf{r}_j'\right)dm_j \\ &\quad - \int_{B_j}\left(\mathbf{1}\times\mathbf{r}_j'\right)^c\cdot\left(\mathbf{1}\times\mathbf{r}_j'\right)\cdot(\mathbf{1}\times\boldsymbol{\omega}_j)dm_j \\ &= \boldsymbol{\omega}_j\times\mathbf{J}_j - \mathbf{J}_j\times\boldsymbol{\omega}_j\end{aligned} \tag{28}$$

in which the formula $\dot{\mathbf{r}}_j' = \boldsymbol{\omega}_j\times\mathbf{r}_j'$ has been used. Furthermore, the substitution of (18) into the previous formula gives rise to

$$\dot{\mathbf{J}}_j = \sum_{k=1}^{m}(\boldsymbol{\varpi}_{jk}\times\mathbf{J}_j - \mathbf{J}_j\times\boldsymbol{\varpi}_{jk})\dot{y}_k. \tag{29}$$

Equation (27) is then rewritten as

$$\begin{aligned}\Pi_{rs} &= \sum_{j=1}^{N}(m_j\dot{\boldsymbol{\gamma}}_{jr}\cdot\boldsymbol{\gamma}_{js} - m_j\boldsymbol{\gamma}_{jr}\cdot\dot{\boldsymbol{\gamma}}_{js}) \\ &\quad + \sum_{j=1}^{N}(\dot{\boldsymbol{\varpi}}_{jr}\cdot\mathbf{J}_j\cdot\boldsymbol{\varpi}_{js} - \boldsymbol{\varpi}_{jr}\cdot\mathbf{J}_j\cdot\dot{\boldsymbol{\varpi}}_{js}) \\ &\quad - \sum_{j=1}^{N}\sum_{k=1}^{m}\boldsymbol{\varpi}_{jr}\cdot(\boldsymbol{\varpi}_{jk}\times\mathbf{J}_j + \mathbf{J}_j\times\boldsymbol{\varpi}_{jk})\cdot\boldsymbol{\varpi}_{js}\dot{y}_k.\end{aligned} \tag{30}$$

Since $\mathbf{J}_j$ is symmetric and $\boldsymbol{\varpi}_{jk}\times\mathbf{J}_j + \mathbf{J}_j\times\boldsymbol{\varpi}_{jk}$ is skew-symmetric, it follows that $\boldsymbol{\Pi}$ is skew-symmetric. □

C. Dynamical Equations of Tri-Wheeled Mobile Robot

For the robot depicted in Fig. 1, the nonholonomic conditions in (7)–(10) may be rewritten in the form of (15), with the 4×6 coefficient matrix $\mathbf{D}$ given by

$$\mathbf{D} = \begin{pmatrix} \sin\theta & -\cos\theta & 0 & 0 & 0 & 0 \\ \cos\theta & \sin\theta & -b & -a & 0 & 0 \\ \cos(\theta+\phi) & \sin(\theta+\phi) & \rho\sin\phi & 0 & -a & 0 \\ \sin(\theta+\phi) & -\cos(\theta+\phi) & -\rho\cos\phi & 0 & 0 & 0 \end{pmatrix}.$$

The velocity corresponding to the sixth column, i.e., $\dot{\phi}$, must be chosen as a privileged velocity, otherwise $\mathbf{D}'$ in (16) becomes singular. Since the tri-wheeled mobile robot is driven by the front wheel, one may choose $\dot{\varphi}_3$ as the other privileged velocity, such that $\dot{\mathbf{y}} = [\dot{\varphi}_3\ \dot{\phi}]^T$. According to this setting, (16) for the nonprivileged velocities $\dot{\mathbf{z}} = [\dot{x}_r\ \dot{y}_r\ \dot{\theta}\ \dot{\varphi}_1]^T$ can be derived, which leads to (17) with coefficient matrix $\mathbf{A}$ given by

$$\mathbf{A} = \begin{pmatrix} a\cos\theta\cos\phi & a\sin\theta\cos\phi & \eta_a\sin\phi & \cos\phi-\eta_b\sin\phi & 1 & 0 \\ 0 & 0 & 0 & 0 & 0 & 1 \end{pmatrix}^T$$

where $\eta_a = a/\rho$ and $\eta_b = b/\rho$.

Substituting the previous expression of $\mathbf{A}$ into (19) and applying (6), the vector $\boldsymbol{\gamma}_{ik}$ are found to be

$$\begin{aligned}\boldsymbol{\gamma}_{1\varphi_3} &= a\cos\theta(\cos\phi-\eta_b\sin\phi)\mathbf{E}^x \\ &\quad + a\sin\theta(\cos\phi-\eta_b\sin\phi)\mathbf{E}^y, \quad \boldsymbol{\gamma}_{1\phi} = 0 \\ \boldsymbol{\gamma}_{2\varphi_3} &= a\cos\theta(\cos\phi+\eta_b\sin\phi)\mathbf{E}^x \\ &\quad + a\sin\theta(\cos\phi+\eta_b\sin\phi)\mathbf{E}^y, \quad \boldsymbol{\gamma}_{2\phi} = 0 \\ \boldsymbol{\gamma}_{3\varphi_3} &= a\cos(\theta+\phi)\mathbf{E}^x + a\sin(\theta+\phi)\mathbf{E}^y, \quad \boldsymbol{\gamma}_{3\phi} = \boldsymbol{\gamma}_{4\phi} = 0 \\ \boldsymbol{\gamma}_{4\varphi_3} &= a\left(\cos\theta\cos\phi - \frac{\rho_r}{\rho}\sin\phi\sin\theta\right)\mathbf{E}^x \\ &\quad + a\left(\sin\theta\cos\phi + \frac{\rho_r}{\rho}\cos\theta\sin\phi\right)\mathbf{E}^y.\end{aligned}$$

On the other hand, the $\boldsymbol{\varpi}_{ik}$ in (19) can be derived from (11) as

$$\begin{aligned}\boldsymbol{\varpi}_{1\varphi_3} &= \eta_a\sin\phi\mathbf{k}_1'' + (\cos\phi-\eta_b\sin\phi)\mathbf{j}_1'', \quad \boldsymbol{\varpi}_{1\phi} = 0 \\ \boldsymbol{\varpi}_{2\varphi_3} &= \eta_a\sin\phi\mathbf{k}_2'' + (\cos\phi+\eta_b\sin\phi)\mathbf{j}_2'', \quad \boldsymbol{\varpi}_{2\phi} = 0 \\ \boldsymbol{\varpi}_{3\varphi_3} &= \eta_a\sin\phi\mathbf{k}_3'' + \mathbf{j}_3'', \quad \boldsymbol{\varpi}_{3\phi} = \mathbf{k}_3'' \\ \boldsymbol{\varpi}_{4\varphi_3} &= \eta_a\sin\phi\mathbf{k}_4'', \quad \boldsymbol{\varpi}_{4\phi} = 0.\end{aligned}$$

Here, the index k for the privileged velocity is changed to the original symbol to enhance the readability.

From the physical description in Section II, the applied forces and torques acting on each rigid body are given by

$$\begin{aligned}&\mathbf{F}_1^a = \mathbf{F}_2^a = \mathbf{F}_3^a = -m_w g\mathbf{E}^z, \quad \mathbf{F}_4^a = -m_p g\mathbf{E}^z, \\ &\mathbf{T}_1^a = 0, \quad \mathbf{T}_2^a = 0, \quad \mathbf{T}_3^a = \tau_1\mathbf{j}_3'' + \tau_2\mathbf{k}_3'', \quad \mathbf{T}_4^a = 0.\end{aligned}$$

Substituting the moments of inertia dyadic given in (3) and (4) and the vectors $\boldsymbol{\gamma}_{ik}$ and $\boldsymbol{\varpi}_{ik}$ into (24), (25), and (26), the reduced Appell equation of tri-wheeled mobile robot in matrix form (23) is deduced with $\mathbf{T}(\mathbf{y}) = \mathbf{B}(\mathbf{y})\boldsymbol{\tau}$ and

$$\begin{aligned}\mathbf{M}(\mathbf{y}) &= \begin{bmatrix} \eta_a^2 I_1\sin^2\phi + I_2\cos^2\phi + I_3 & \eta_a I_m\sin\phi \\ \eta_a I_m\sin\phi & I_m \end{bmatrix} \\ \mathbf{C}(\mathbf{y},\dot{\mathbf{y}}) &= \begin{bmatrix} 0.5(\eta_a^2 I_1 - I_2)\dot{\phi}\sin 2\phi & 0 \\ \eta_a I_m\dot{\phi}\cos\phi & 0 \end{bmatrix} \\ \mathbf{B}(\mathbf{y}) &= \begin{bmatrix} 1 & \eta_a\sin\phi \\ 0 & 1 \end{bmatrix} \\ I_1 &= \left(3I_m + I_p + 4(b/a)^2 I_m + 2m_w b^2 + m_p\rho_r^2\right), \\ I_m &= m_w' a^2/2 \\ I_2 &= \left(4I_m + 2m_w a^2 + m_p a^2\right) \\ I_3 &= (m_w a^2 + 2I_m), \quad I_p = m_p'(w^2+l^2)/3.\end{aligned} \tag{31}$$

It can be checked directly that *Lemmas 1* and *2* are indeed satisfied.

While one may adopt the Lagrangian formulation to obtain the equations of motion of the same form, the previous process of derivation is much more systematic, and reveals the intrinsic structure of a complex multibody system subject to nonholonomic constraints. Note that the nonprivileged variables $\mathbf{z}$ do not appear in (31). Hence, the system of tri-wheeled mobile robots is reducible, after the subtle selection of the set of privileged variables.

Authorized licensed use limited to: National Taiwan University. Downloaded on December 19, 2008 at 02:28 from IEEE Xplore. Restrictions apply.

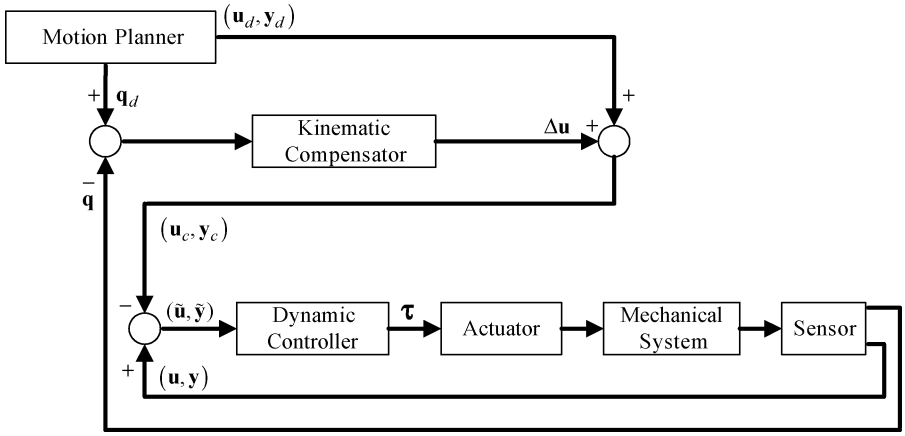

Fig. 3. Block diagram of hierarchical control design.

IV. Design of Hierarchical Controller

A. General Methodology

The reduced Appell equation (21) and the kinematic equation (16) together govern the dynamics of the tri-wheeled robot. Since the former equation for $\mathbf{y}$ are decoupled from the latter one, a controller to steer $\mathbf{y}$ follow the desired $\mathbf{y}_d(t)$ may be designed individually. However, the desired $\mathbf{z}_d(t)$ may not be tracked if the initial condition is not perfect, or disturbances occur during the motion without taking (16) into consideration. To take advantage of the decoupling feature of the system, a hierarchical tracking control scheme is proposed, with its block diagram being shown in Fig. 3.

On the top level, the motion planner produces the desired trajectory $\mathbf{q}_d(t) = [x_{rd}(t)\ y_{rd}(t)\ \theta_d(t)\ \varphi_{1d}(t)\ \varphi_{3d}(t)\ \phi_d(t)]^T$ based on task requirements and the conditions of constraints. The tracking of $\mathbf{z}_d(t)$ is achieved by changing the desired privileged velocities $\mathbf{u}_d\ (= \dot{\mathbf{y}}_d)$ to $\mathbf{u}_c = \mathbf{u}_d + \Delta\mathbf{u}$, where $\Delta\mathbf{u}$ is computed through a kinematic compensator in the middle level. The updated desired privileged coordinates are then found, $\mathbf{y}_c = \mathbf{y}_d + \Delta_{\mathbf{y}}$, where $\Delta\mathbf{y} = \int \Delta\mathbf{u}$, which is fed along with $\mathbf{u}_c$ to the dynamical controller in the bottom level to drive the mobile robot.

It is noted that the information of all generalized coordinates are needed in the middle level, while only those of the privileged ones are required in the bottom level. This feature due to decoupling makes it possible to run the hierarchical controller at different sampling rates. In particular, for the mobile robot system, the kinematic compensator may use slower sensors such as the global positioning system (GPS) to locate the robot, and faster sensors such as the encoders may be implemented with the dynamic controller. It shall be shown later by simulation that the proposed hierarchical controller with different sampling rates is feasible.

We now apply the concept of the hierarchical control to drive the tri-wheeled mobile robot along a desired trajectory. In terms of $u_1 = \dot{\varphi}_3$ and $u_2 = \dot{\phi}$, the kinematic equation becomes

$$\begin{cases} \dot{x}_r = a u_1 \cos\theta \cos\phi \\ \dot{y}_r = a u_1 \sin\theta \cos\phi \\ \dot{\theta} = \eta_a u_1 \sin\phi \\ \dot{\phi} = u_2. \end{cases} \tag{32}$$

It can be checked that the above system with system variables (x_r, y_r, θ, ϕ) is differentially flat with two output variables (x_r, y_r), cf. [20]. For given $x_{rd}(t)$, $y_{rd}(t)$, we have $\theta_d = \tan^{-1}(\dot{y}_{rd}/\dot{x}_{rd})$, $\phi_d = \tan^{-1}(\rho\omega_d/v_d)$, where the reference values for the linear velocity and the angular velocity are, respectively

$$v_d = \sqrt{\dot{x}_{rd}^2 + \dot{y}_{rd}^2}, \qquad \omega_d = \frac{\ddot{y}_{rd}\dot{x}_{rd} - \ddot{x}_{rd}\dot{y}_{rd}}{\dot{x}_{rd}^2 + \dot{y}_{rd}^2}.$$

The kinematic compensator is then realized by a fuzzy logic system to infer the compensations $\Delta v, \Delta\omega$. Since $v = a\dot{\varphi}_3 \cos\phi$ and $\omega = (a/\rho)\dot{\varphi}_3 \sin\phi$, a new set of reference values for the privileged variables are then computed as

$$\mathbf{u}_c = \left(\sqrt{\left(\frac{\Delta v + v_d}{a}\right)^2 + \left(\frac{\rho(\Delta\omega + \omega_d)}{a}\right)^2}, \ \frac{d}{dt}\left(\tan^{-1}\frac{\rho(\Delta\omega + \omega_d)}{(\Delta v + v_d)}\right) \right) \tag{33}$$

$$\mathbf{y}_c = \left(\int \sqrt{\left(\frac{\Delta v + v_d}{a}\right)^2 + \left(\frac{\rho(\Delta\omega + \omega_d)}{a}\right)^2}, \ \tan^{-1}\frac{\rho(\Delta\omega + \omega_d)}{(\Delta v + v_d)} \right) \tag{34}$$

which is fed into a sliding-mode controller to track the corrected desired values, cf. Section IV-C.

B. Fuzzy Logic Compensator in Kinematic Level

In steering a mobile robot, the position and the heading (namely, the posture) of the platform are the key variables to be tracked. The deviation of the current posture to the desired one can be represented by, cf. Fig. 4

$$\begin{bmatrix} \xi_e \\ \eta_e \\ \theta_e \end{bmatrix} = \begin{bmatrix} \cos\theta & \sin\theta & 0 \\ -\sin\theta & \cos\theta & 0 \\ 0 & 0 & 1 \end{bmatrix} \begin{bmatrix} x_{rd} - x_r \\ y_{rd} - y_r \\ \theta_d - \theta \end{bmatrix}. \tag{35}$$

Denote the length of the vector from the current position to the desired one by $d_e = \sqrt{\xi_e^2 + \eta_e^2}$, and the corresponding angle by $\vartheta_e = \tan^{-1}(\eta_e/\xi_e)$. The latter shall be termed the *line-of-sight angle*, and is different from the heading angle error θ_e. To reduce these errors, so that the nonprivileged coordinates in the set of system variables can be tracked, a fuzzy logic system is designed to serve as a kinematic

Authorized licensed use limited to: National Taiwan University. Downloaded on December 19, 2008 at 02:28 from IEEE Xplore. Restrictions apply.

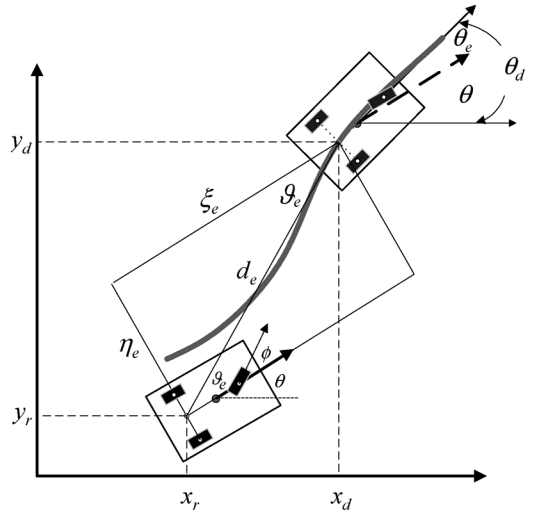

Fig. 4. Current versus desired configuration of the mobile robot.

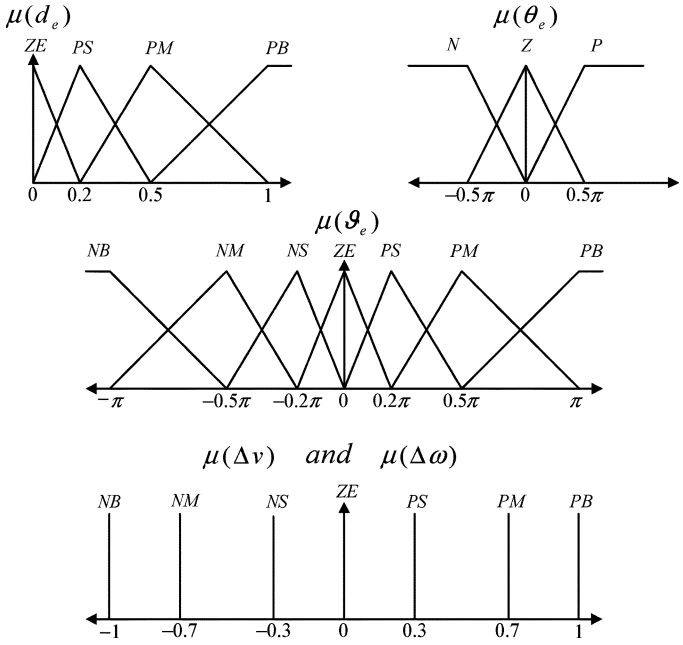

Fig. 5. Membership functions of input and output variables.

compensator. Similar ideas have been used in [21], among others, in dealing with the autonomous vehicle navigation problems.

In the design, the sets of input and output variables are selected to be $(d_e, \vartheta_e, \theta_e)$ and $(\Delta v, \Delta\omega)$, respectively. According to drivers' experiences, the membership functions for these variables after scaling by suitable factors are chosen as those shown in Fig. 5. The symbols Z, P, N, S, M, B represent zero, positive, negative, small, medium, big, respectively. Based on these membership functions, a total of 28×3 inference rules are used to find the intermediate values of Δv and $\Delta\omega$, as listed in Table I. The final compensations are determined by invoking the defuzzification process with the center-of-gravity scheme.

It is noted that both θ_e and ϑ_e are taken into account in the design. This is because if only θ_e is considered, the line-of-sight angle can not be adjusted and the vehicle may trace a trajectory parallel to the reference one. On the other hand, if only ϑ_e is included, the compensated value $\Delta\omega$ may exhibit a chattering phenomenon, which may lead to zig-zag motions of the vehicle. The concept of line-of-sight angle has been used frequently in proportional navigation for ballistic missiles [22]. Its inclusion in the algorithm here can significantly reduce the steady-state errors.

C. Adaptive Sliding-Mode Control in Dynamic Level

After scaling the compensations Δv, $\Delta\omega$ obtained from the fuzzy system, a new set of desired privileged variables is computed from (33) and (34), respectively. They are to be tracked by exerting $\boldsymbol{\tau}$ in the reduced dynamics (23), which is rewritten as

$$\dot{\mathbf{y}} = \mathbf{u}, \mathbf{M}(\mathbf{y})\dot{\mathbf{u}} + \mathbf{C}(\mathbf{y}, \mathbf{u})\mathbf{u} = \mathbf{B}(\mathbf{y})\boldsymbol{\tau} \tag{36}$$

where it is assumed that some parameters such as masses, moments of inertia, and physical specifications, etc., are not known exactly.

To design a controller accommodating the uncertain parameters such that the tracking errors $\tilde{\mathbf{u}}(t) \equiv \mathbf{u}(t) - \mathbf{u}_c(t)$ and $\tilde{\mathbf{y}}(t) \equiv \mathbf{y}(t) - \mathbf{y}_c(t)$ approach zero asymptotically as $t \to \infty$, the idea of adaptive sliding-mode control [23] is applied. In the method, the sliding variable $\mathbf{s}$ is defined as

$$\mathbf{s} = [s_1 \quad s_2]^T = \tilde{\mathbf{u}} + \boldsymbol{\Lambda}\tilde{\mathbf{y}} = \mathbf{u} - \mathbf{u}_s \tag{37}$$

where $\mathbf{u}_s = [u_{s1}\ u_{s2}]^T = [\dot{\varphi}_{3s}\ \dot{\phi}_s]^T = \mathbf{u}_c - \boldsymbol{\Lambda}\tilde{\mathbf{y}}$ and $\boldsymbol{\Lambda}$ is a positive-definite matrix. Let $\boldsymbol{\Theta} = [\eta_a^2 I_1\ I_2\ I_3\ I_m]^T$ be the vector containing uncertain parameters. It can be checked that

$$\mathbf{M}(\mathbf{y})\dot{\mathbf{u}}_s + \mathbf{C}(\mathbf{y}, \mathbf{u})\mathbf{u}_s = \boldsymbol{\Delta}(\mathbf{y}, \mathbf{u}, \mathbf{u}_s, \dot{\mathbf{u}}_s)\boldsymbol{\Theta} \tag{38}$$

where the regressor matrix $\boldsymbol{\Delta}$ in the above linear parametric form [11] is given by the equation shown at the bottom of the page.

From (36) and (38), the evolution equation of the sliding variable is found to be

$$\mathbf{M}(\mathbf{y})\dot{\mathbf{s}} + \mathbf{C}(\mathbf{y}, \mathbf{u})\mathbf{s} = \mathbf{B}(\mathbf{y})\boldsymbol{\tau} - \boldsymbol{\Delta}(\mathbf{y}, \mathbf{u}, \mathbf{u}_s, \dot{\mathbf{u}}_s)\boldsymbol{\Theta}. \tag{39}$$

The problem is then converted to find $\boldsymbol{\tau}$, which depends on the unknown parameter vector $\boldsymbol{\Theta}$, such that $\mathbf{s} \to \mathbf{0}$. Let $\hat{\boldsymbol{\Theta}}$ denote the estimate of $\boldsymbol{\Theta}$. By adopting the following control and adaptive laws:

$$\begin{cases} \boldsymbol{\tau} = \mathbf{B}^{\#}(\mathbf{y})\left[\boldsymbol{\Delta}(\mathbf{y}, \dot{\mathbf{y}}, \mathbf{u}_s, \dot{\mathbf{u}}_s)\hat{\boldsymbol{\Theta}} - \mathbf{K}_s\mathbf{s}\right] \\ \dot{\hat{\boldsymbol{\Theta}}} = -\boldsymbol{\Gamma}^{-1}\boldsymbol{\Delta}(\mathbf{y}, \dot{\mathbf{y}}, \mathbf{u}_s, \dot{\mathbf{u}}_s)^T\mathbf{s} \end{cases} \tag{40}$$

where $\mathbf{K}_s$ and $\boldsymbol{\Gamma}$ are positive-definite matrices, and $\mathbf{B}^{\#}$ is the left inverse of $\mathbf{B}$, one can show by Lyapunov analysis [24] that $\mathbf{u} \to \mathbf{u}_c$ and $\mathbf{y} \to \mathbf{y}_c$ asymptotically. It is seen that the nonprivileged variables in

$$\begin{bmatrix} \dot{u}_{s1}\sin^2\phi & \dot{u}_{s1}\cos^2\phi & & \\ +0.5u_{s1}u_2\sin 2\phi & -0.5u_{s1}u_2\sin 2\phi & \dot{u}_{s1} & \eta_a\dot{u}_{s2}\sin\phi \\ 0 & 0 & 0 & \eta_a\dot{u}_{s1}\sin\phi + \dot{u}_{s2} + \eta_a u_{s1}u_2\cos\phi \end{bmatrix}$$

Authorized licensed use limited to: National Taiwan University. Downloaded on December 19, 2008 at 02:28 from IEEE Xplore. Restrictions apply.

TABLE I
FUZZY RULES FOR KINEMATIC COMPENSATOR

θ_e		d_e							
		ZE		PS		PM		PB	
ϑ_e		Δv	$\Delta\omega$	Δv	$\Delta\omega$	Δv	$\Delta\omega$	Δv	$\Delta\omega$
PB		ZE	ZE	NS	PM	NM	PS	NB	ZE
		ZE	PS	ZE	PM	NS	PS	NM	ZE
		ZE	NS	ZE	PM	NS	PS	NM	ZE
		ZE	ZE	PM	PM	NS	PS	NM	ZE
PM		ZE	ZE	PS	PM	PS	PS	PM	ZE
		ZE	PS	ZE	PM	ZE	PS	PS	ZE
		ZE	NS	ZE	PM	ZE	PS	PS	ZE
		ZE	ZE	PM	PM	ZE	PS	PS	ZE
PS		ZE	ZE	PS	PM	PM	ZE	PB	ZE
		ZE	PS	PS	PS	PS	ZE	PM	ZE
		ZE	NS	PS	PS	PS	ZE	PM	ZE
		ZE	ZE	PS	PS	PS	ZE	PM	ZE
ZE		ZE	ZE	PS	ZE	PM	ZE	PB	ZE
		ZE	PS	PS	ZE	PM	ZE	PB	ZE
		ZE	NS	PS	ZE	PM	ZE	PB	ZE
		ZE	ZE	PS	ZE	PM	ZE	PB	ZE
NS		ZE	ZE	PS	NS	PM	ZE	PB	ZE
		ZE	PS	PS	NS	PS	ZE	PM	ZE
		ZE	NS	PS	NS	PS	ZE	PM	ZE
		ZE	ZE	PS	NS	PS	ZE	PM	ZE
NM		ZE	ZE	PS	NM	PS	NS	PM	ZE
		ZE	PS	ZE	NM	ZE	NS	PS	ZE
		ZE	NS	ZE	NM	ZE	NS	PS	ZE
		ZE	ZE	ZE	NM	ZE	NS	PS	ZE
NB		ZE	ZE	NS	NM	NM	NS	NB	ZE
		ZE	PS	ZE	NM	NS	NS	NM	ZE
		ZE	NS	ZE	NM	NS	NS	NM	ZE
		ZE	ZE	ZE	NM	NS	NS	NM	ZE

$\mathbf{z}$ do not appear in (40), and hence, the dynamic controller can operate without the information of $\mathbf{z}$.

V. SIMULATION RESULTS

To examine the effectiveness of the proposed hierarchical control strategy, computer simulations were performed. The system parameters of a large mobile robot shown in Fig. 2 are selected as $a = 0.3$ m, $\rho_r = 0.5$ m, $\rho_f = 0.75$ m, $l = 1.75$ m, $w = 1.5$ m, $m_p = 20$ kg, $m_p' = 6$ kg, $m_w = 1$ kg, $m_w' = 2$ kg. The desired trajectory $(x_{rd}(t), y_{rd}(t))$ is first obtained by finding a cubic B-spline curve, cf. [25], passing through 11 intermediate points, {(0,0), (2,9), (5,16), (9,20), (13,18), (14.5,15), (17,11), (22,13), (22,20), (17,22), (13,18)}. Next, the desired values of other system variables $(\theta_d(t), \phi_d(t))$ are computed. Based on the current status of the vehicle, the fuzzy inference engine discussed in Section IV-B with rules given in Table I is then invoked. The scale of Δv is proportional to v_d with factor 0.6, while that of $\Delta\omega$ is inversely proportional to v_d with factor 5. The compensations $\mathbf{u}_c$ and $\mathbf{y}_c$ are then computed from (33) and (34), and fed into the sliding-mode tracking controller described in Section IV-C. The parameters in the control scheme and adaptive law (40) are chosen by testing as $\mathbf{K}_s = \mathrm{diag}\{10, 10\}$, $\Lambda = \mathrm{diag}\{4, 4\}$, $\Gamma = \mathrm{diag}\{20, 10, 100, 1000\}$ to assure appropriate convergence rates. In the adaptive scheme, the initial condition $\hat{\mathbf{\Theta}}(0) = [0.1 \;\; 0.1 \;\; 0.1 \;\; 0.001]^T$ is used, which is different from the true value $\mathbf{\Theta}_{\mathrm{true}} = [1 \;\; 2.3 \;\; 0.3 \;\; 0.09]^T$. Moreover, we set the initial posture as $x_r(0) = 10, y_r(0) = 0$, and $\theta(0) = 0^o$, comparing with the desired values $(0, 0, 45^o)$.

For the above-described scenario, simulations were performed such that the kinematic compensator, the dynamic controller, and the system simulator were executed in different sampling rates: 10 Hz, 100 Hz, and 1 kHz, respectively. The results are shown in Figs. 6 and 7. In Fig. 6, the solid line is the desired B-spline curve, and the shaded block line shows the tracking performance. It is observed that while the initial condition is significantly away from the desired configuration in both position and heading, the proposed hierarchical controller can successfully steer the mobile robot back to the desired trajectory. The tracking errors of the system variables (x_r, y_r, θ, ϕ) are plotted in Fig. 7. It is seen that not only the errors of the privileged coordinates, but also those of the non-privileged coordinates, in the set of system variables are driven asymptotically to zero. Furthermore, simulations were also conducted in the presence of sensor errors, such as 10 cm in position and 5° in angle, for which the hierarchical controller works quite well.

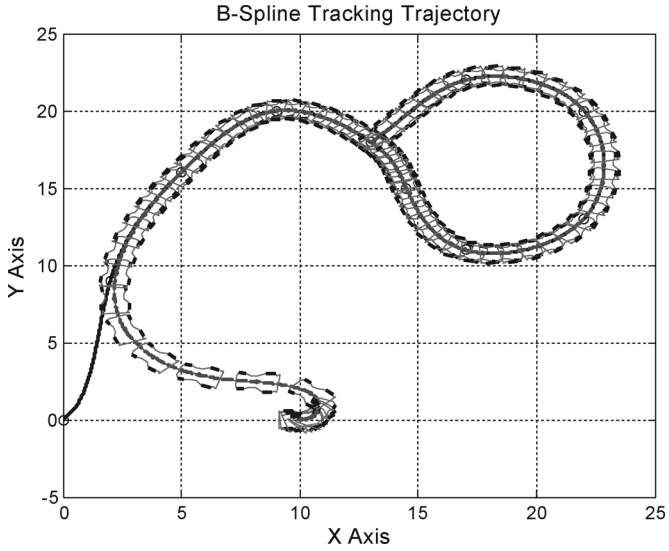

Fig. 6. B-spline tracking trajectory.

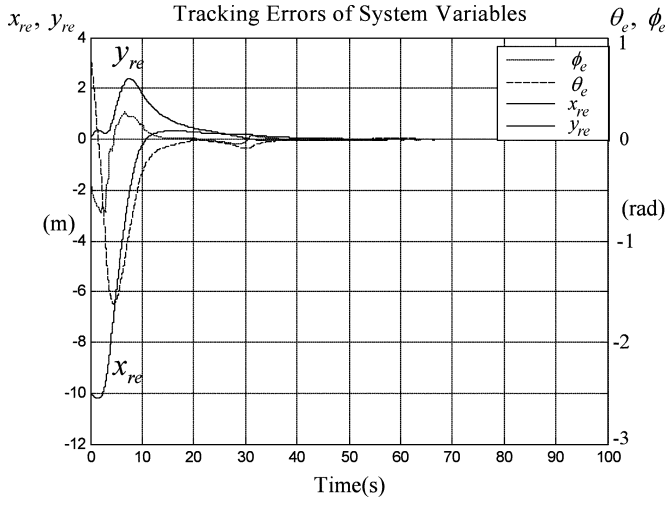

Fig. 7. Tracking error of system variables.

Authorized licensed use limited to: National Taiwan University. Downloaded on December 19, 2008 at 02:28 from IEEE Xplore. Restrictions apply.

VI. Conclusions

In this paper, a hierarchical tracking controller was designed for a tri-wheeled mobile robot based on the model established using Appell's equation. Taking advantage of the decoupling feature of the system, all the system variables can be steered to their respective desired values, even if there are some unknown parameters and measurement errors. Incorporating the practical driving experiences in the design of fuzzy rules, the reference trajectory for the dynamic controller is changed through the kinematic compensator. The skew-symmetric property of the reduced Appell equation proved in Section III assures that the selected adaptive controller can asymptotically steer the privileged variables. This methodology successfully integrates the kinematic constraints and the dynamics to generate practical control command to the mechanical system. Based on our design, it is possible to run the controller and the compensator at different sampling rates, as shown in Section V, which may not be feasible for the previous designs of two-stage controllers, such as in [10] and [11].

The success of the hierarchical design proposed here relies heavily on the decoupling of the dynamical equations from the kinematic constraints. The separation of coordinates in the early stage into privileged versus nonprivileged ones is essential to the design. Using of the structured form of the Appell equation not only reduces the complexity in the modeling of coupled mechanical systems, but also helps to establish a suitable model for control. This shows the merit of closely integrating the methods of mechanics and those of controls in robotics. One may also adopt other types of controllers, such as a neural network controller or robust controller, to steer the privileged variables or to compute the compensations. Applications of the proposed method to more complicated mechanical systems using various types of controllers are currently under investigation.

References

[1] I. Kolmanovsky and N. H. McClamroch, "Developments in non-holonomic control problems," *IEEE Control Systems Mag.*, vol. 15, no. 6, pp. 20–36, 1995.

[2] R. M. Murray and S. S. Sastry, "Nonholonomic motion planning: Steering using sinusoids," *IEEE Trans. Autom. Control*, vol. 38, no. 5, pp. 700–716, May 1993.

[3] G. Paolo and G. Alessandro, "A technique to analytically formulate and to solve the 2-dimensional constrained trajectory planning problem for a mobile robot," *J. Intell. Robot. Syst.*, vol. 27, pp. 237–262, 2000.

[4] A. Astolfi, "Exponential stabilization of a car-like vehicle," in *Proc. IEEE Int. Conf. Robot. Autom.*, 1995, pp. 1391–1396.

[5] J. Guldner and V. I. Utkin, "Sliding mode control for gradient tracking and robot navigation using artificial potential fields," *IEEE Trans. Robot. Autom.*, vol. 11, no. 2, pp. 247–254, Apr. 1995.

[6] C. Samson, "Control of chained system: Application to path following and time-varying point-stabilization of mobile robots," *IEEE Trans. Autom. Control*, vol. 40, no. 1, pp. 64–77, Jan. 1995.

[7] Z. P. Jiang and H. Nijmeijer, "A recursive technique for tracking control of nonholonomic systems in chained form," *IEEE Trans. Autom. Control*, vol. 44, no. 2, pp. 265–279, Feb. 1999.

[8] O. J. Sørdalen and O. Egeland, "Exponential stabilization of nonholonomic chained systems," *IEEE Trans. Autom. Control*, vol. 40, no. 1, pp. 35–49, Jan. 1995.

[9] R. Fierro and L. Lewis, "Practical point stabilization of a nonholonomic mobile robot using neural networks," in *Proc. 35th IEEE Conf. Decision, Control*, 1996, pp. 1722–1727.

[10] W. Dong and W. Huo, "Adaptive stabilization of uncertain dynamic non-holonomic systems," *Int. J. Control*, vol. 72, no. 18, pp. 1689–1700, 1999.

[11] S. S. Ge and G. Y. Zhou, "Adaptive robust stabilization of dynamic nonholonomic chained systems," *J. Robot. Syst.*, vol. 18, no. 3, pp. 119–133, 2001.

[12] S. Lin and A. Goldenberg, "Robust damping control of wheeled mobile robot," in *Proc. IEEE Int. Conf. Robot. Autom.*, 2000, pp. 2919–2924.

[13] T. R. Kane and J. Levinson, "Formulation of equations of motion for complex spacecraft," *J. Guid. Control*, vol. 3, no. 2, pp. 99–112, 1980.

[14] P. E. B. Jourdain, "Note on an analogue of Gauss' principle of least constraint," *Q. J. Pure Appl. Math.*, vol. 8, pp. 153–157, 1909.

[15] L. S. Wang and Y. H. Pao, "Jourdain's variational equation and Appell's equation of motion for nonholonomic dynamical systems," *Amer. J. Phys.*, vol. 71, no. 1, pp. 72–82, 2003.

[16] T. R. Kane, "Dynamics of nonholonomic systems," *J. Appl. Mech.*, vol. 83, pp. 574–578, 1961.

[17] C. E. Weatherburn, *Elementary Vector Analysis: With Application to Geometry and Physics*. London, U.K.: G. Bell, 1921.

[18] L. A. Pars, *A Treatise on Analytical Dynamics*. Woodbridge, CT: Ox Bow Press, 1965.

[19] J. L. Junkins, Ed., *Mechanics and Control of Large Flexible Structures*. Washington, DC: AIAA, 1990.

[20] M. Fliess, J. Lévine, P. Martin, and P. Rouchon, "On differentially flat nonlinear systems," in *Proc. IFAC Symp. Nonlinear Control Syst. Des.*, 1992, pp. 408–412.

[21] D. Driankov and A. Saffiotti, *Fuzzy Logic Techniques for Autonomous Vehicle Navigation*. New York: Physica-Verlag, 2001.

[22] D. Ghose, "True proportional navigation with maneuvering target," *IEEE Trans. Aerosp. Electron. Syst.*, vol. 30, no. 1, pp. 229–237, Jan. 1994.

[23] V. I. Utkin, "Variable structure systems with sliding modes," *IEEE Trans. Autom. Control*, vol. AC-22, no. 2, pp. 212–222, Feb. 1977.

[24] K. Y. Lian, L. S. Wang, and L. C. Fu, "Globally valid adaptive controllers of mechanical systems," *IEEE Trans. Autom. Control*, vol. 42, no. 8, pp. 1149–1154, Aug. 1997.

[25] P. S. Tsai, L. S. Wang, F. R. Chang, and T. F. Wu, "Systematic backstepping design for B-spline trajectory tracking control of the mobile robot in hierarchical model," in *Proc. IEEE Int. Conf. Netw., Sensing, Control*, 2004, pp. 713–718.

Stability Analysis of a Vision-Based Control Design for an Autonomous Mobile Robot

Jean-Baptiste Coulaud, Guy Campion, Georges Bastin, and Michel De Wan

***Abstract*—We propose a simple control design allowing a mobile robot equipped with a camera to track a line on the ground. The control algorithm, as well as the image-processing algorithm, are very simple. We discuss the existence and the practical stability of an equilibrium trajectory of the robot when tracking a circular reference line. We then give a complementary analysis for arbitrary reference lines with bounded curvature. Experimental results confirm the theoretical analysis.**

***Index Terms*—Control-design analysis, mobile robot, path tracking, visual servoing.**

I. Introduction

The problem addressed in this paper is the feedback-control design allowing a mobile robot to track a line on the ground using visual feedback. There exist a lot of image-processing algorithms extracting

Manuscript received September 8, 2005; revised January 23, 2006. This paper was recommended for publication by Associate Editor D. Prattichizzo and Editor L. Parker upon evaluation of the reviewers' comments. This paper was presented in part at the 16th IFAC World Congress, Prague, Czech Republic, July 2005. Color versions of Figs. 1–12 are available online at http://ieeexplore.org. This paper presents research results of the Belgian Programme on Interuniversity Attraction Poles, initiated by the Belgian Federal Science Policy Office. The scientific responsibility rests with its authors.

The authors are with the CESAME/UCL, B1348 Louvain-La-Neuve, Belgium (e-mail: coulaud@inma.ucl.ac.be; campion@inma.ucl.ac.be; bastin@inma.ucl.ac.be; dewan@inma.ucl.ac.be).

Color versions of Figs. 1–12 are available online at http://ieeexplore.ieee.org.

Digital Object Identifier 10.1109/TRO.2006.878934

Authorized licensed use limited to: National Taiwan University. Downloaded on December 19, 2008 at 02:28 from IEEE Xplore. Restrictions apply.